Supplement to: Improving the accuracy in particle concentration measurements of a balloon-borne optical particle counter UCASS

Sina Jost[1], Ralf Weigel[1], Konrad Kandler[2], Luis Valero[2], Jessica Girdwood[3, 4], Chris Stopford[3], Warren Stanley[3], Luca K. Eichhorn[1], Christian von Glahn[1], and Holger Tost[1]

[1]Institute for Physics of the Atmosphere, Johannes Gutenberg University, Mainz, Germany

[2]Institute for Applied Geosciences, Technical University Darmstadt, Germany

[3]Particle Instruments & Diagnostics Research Group, University of Hertfordshire, Hatfield, Hertfordshire, AL10 9AB, United Kingdom

[4]National Centre for Atmospheric Science, School of Earth, Atmospheric and Environmental Sciences, University of Manchester, Manchester, M13 9PL, United Kingdom

Corresponding authors: Sina Jost (sjost@students.uni-mainz.de) and Ralf Weigel, (weigelr@uni-mainz.de)

S 1 TFS performance, cold chamber tests

To operate the TFS in general, it was installed onto a custom-designed Printed Circuit Board (PCB9, Fig. S 1), allowing powering the sensor (by a 12 V DC power supply) and reading the voltage output (U) with a multimeter. For the cold chamber test, two TFS were mounted opposite each other in a flow tube of 1015 mm total length, 110 mm diameter, in a distance to tube inlet 820 mm. The sensors measured inside the tube at a distance of 30 mm from the inner tube wall. The PPt was placed at the same position on the longitudinal axis of the flow tube (PPt tip at 820 mm downstream of the tube inlet), but radially offset by 90° to the TFS and about 35 mm into the pipe interior. The PPt was operated in STP mode, i.e. the manually set temperature conditions were directly output as STP-corrected velocities in the PPt control unit (TSI Inc., model 8710 plus). The TFS had been individually calibrated against the PPt in the horizontal wind tunnel (see main article, Sect. 3.5.3 and 4.1) prior to the cold chamber experiment. The TFS voltages were translated according to the calibration function and also STP-density corrected. The resulting velocity values of the two TFSs were compared with those of the PPt for at least 41 (up to a maximum of 78) individual measurements per ambient temperature of 19°, 10°, 0°, -5°, -10°, -15°, and -20°C.

The ratios of the velocities – determined from the TFS measurement and the reference measurement (PPt) – as a function of the ambient temperature are shown in Fig. S 2:

1) For TFS 1 a systematic offset is visible (Fig. S 2; potentially due to a) the previously performed calibration, b) any mistreatment since these calibrations, or c) the installation in the flow tube for the cold test).

2) For TFS 2 a higher variability was observed as a function of ambient temperature (Fig. S 2), but the data remain comparatively close to the 1:1 ratio.

No temperature-related trend can be determined from the data that could be interpreted as a temperature-effect on the TFS electronics and that could be corrected. The normalization of the TFS to the reference measurement remains almost constant. Hence, the temperature has minor effect on one sensor and in a repeated measurement, we could only determine a temperature-related increase in the measurement uncertainty ($1.96 \cdot \sigma$) from about ± 10 % (as read from Fig. S 2 at ambient temperatures above 0°C) to up to about ± 15 % (at ambient temperatures below 0°C) for the TFS measurement.

S 2 Extended TFS calibrations

Figure S 7 shows an example of the TFS 8 calibration with the measured TFS output voltage versus the PPt-measured flow velocity. The standard deviation (σ) of the TFS voltage ranged between 0.002 and 0.005 V, which corresponds to a percentage of 0.1 to 0.2 % relative to the mean. According to the functional relationship in Eq. 1 (see main article), the data points were fitted, which is used hereafter as the calibration curve of a TFS. For each measuring point, the mean value plus (minus) the associated standard deviation - i.e. the extremes of variability – was inserted into the calibration curve function and the resulting deviation from the pure mean value calibration was determined. The flow velocity based on this calibration curve deviated from the averaged measurement point at the most by 0.08 m s^{-1} corresponding to a percentage maximum of 1.3 %. The σ resulting for measured and averaged v_{PPt} is 0.01 to 0.08 m s^{-1} corresponding to a percentage of 0.3 - 10.4 %, while the relative deviation increased significantly at flow velocities slower than 1.5 m s^{-1}. At higher flows a percentage of 1 % was not exceeded.

As part of the calibrations, further very specific properties of the TFS were analysed in more detail:

- The TFS readings could not be processed with an ambient flow of 0 m s^{-1}, as the values of the same TFS varied differently strong at a zero-measurement depending on the duration the TFS is supplied with voltage prior to the measurements (warm-up time, which varied depending on the TFS).
- A minimum ambient flow should always be present during these calibrations. When using the slowest (non-zero) wind tunnel flow during a high-resolution TFS calibration, the calibration curves of the same TFS (obtained at invariant laboratory conditions, e.g. over one day) reproduced within 1 % for ambient flows of ~ 2 – 8 m s^{-1}. Repeated calibrations with time offset and with the same TFS after disassembly/reassembly also reproduced within 1.8 % at maximum, and on average within 1 %.
- The calibration curves were likely influenced by the ambient conditions in the laboratory, as the temperature and pressure in the laboratory affects air's density, which in turn controls the heat advection at the TFS.

Three calibration points reproduced the high-resolution calibration (HRC) curve already with acceptable accuracy. The procedure is described and compared in the following for TFS 8 and TFS 6.

TFS 8 was aligned with the positioning device and was equipped with a low-pass filter (see main article, Sect. 3.2). As part of the calibration, the mean value of the electrical voltage (TFS) and the mean value of the flow velocity (PPt) were determined for 25 different wind tunnel flow velocities. Figure S 7 shows the measured values with standard deviation and the calibration curve of TFS 8. To determine the calibration curve from three reference points, three measured values were selected from the 25 measured values already recorded. These are marked in grey in Fig. S 8a and should ideally be recorded at ambient flows of 2 m s^{-1}, 5 m s^{-1}, and 8 m s^{-1}. The coefficients of a calibration curve were determined from these three calibration points. The resulting fit is shown in Fig. S 8a as dashed line and is referred to as a three-point calibration (TPC) curve.

For flow velocities of 2-8 m s^{-1}, the TPC curve never deviated by more than 1 % from the initial HRC curve. Visually, the two curves shown in Fig. S 8a are almost congruent. This procedure was carried out and tested for all recorded calibration curves as e.g. for TFS 6 (results shown in Fig. S 8b). In one of several TFS 6 calibration series (not shown herein), a maximum relative percentage deviation of 2.9 % between its HRC and corresponding TPC curve was found at ambient flows between 2 and 8 m s^{-1}. The following reasons were identified as potential causes of this

exceptional case: a) the influence of changed laboratory conditions, b) the fact that TFS 6 was not yet equipped with a low-pass filter at the time of calibration and c) a TFS adjustment without a positioning device. All three reasons may have had overlapping but ultimately unquantifiable individual influences.

S 3 Extended TFS calibrations at variable angle-of-attack (AOA)

The measurement series (main article, Sect. 4.3) were repeated under variable AOA with the UCASS-implemented TFS 7 by using the positioning device for its alignment. Figure S 9 indicates, that the number of different AOA was reduced compared to previous experiments (see main article, Sect. 4.3) and it also shows the results of this experiment repetition.

As the test setup had to be changed during this experiment series, two calibration curves were recorded, one of which was determined before (TFS 7.2, highly resolved) and a second one after (TFS 7.3, three-point calibration) the setup modifications. The relative deviation of the calibration curve TFS 7.3 in reference to the calibration curve TFS 7.2 was at the maximum of 2.5 % for ambient flow velocities between 2 and 8 m s^{-1}, with an average relative deviation of 1.5 %. The standard deviations σ of the two calibrations with TFS 7 were between 0.001 and 0.020 V (TFS 7) and 0.01 and 0.14 m s^{-1} (PPt). As already observed with TFS 8 (main article, Sect. 4.3), the σ-values increased with increasing deflection angle. The error in the angle setting was still estimated at ±0.5° in each case.

The relative percentage deviation (maximum and mean) of UCASS-internal flow velocities at variable AOA in reference to the calibration curves of TFS 7 are given in Table S 2. For AOA up to 20°, a maximum of 1.8 % relative deviation was not exceeded. The relative deviation from the calibration curve increased significantly at deflection angles > 30°. In agreement with the experiment series of the TFS 8, this series of measurements with the TFS 7 also showed decreasing UCASS-internal flow velocities with increasing AOA.

Qualitatively, the measurement series of the TFS 8 were confirmed by those with the TFS 7. Moreover, the maximum and mean deviations of both experiment series were largely reproduced in quantitative terms, predominantly at small deflection angles. However, a few exceptions - particularly at AOA larger than 30° (i.e. 35° or 40°) in each direction - yielded differing results. This may again be due to the possible interference discussed for large deflections (see main article, Sect. 4.3).

S 4 Payload's deflection from the straight vertical

One balloon sounding (11 July 2023, 14:00 CEST) was analysed, which was not related to one of the herein discussed field missions and where no TFS-equipped UCASS was deployed. However, the balloon-payload-ensemble carried two radiosondes (RS41-SGP), one sonde (RS1) was placed directly underneath the balloon hull, the second one (RS2) was attached to the payload. With the parachute (if not unfolded of ~ 2 m length) and with the unwinder's rope length of ~ 60 meters the balloon-payload-structure had a total length of about 62 m. The analysis of both RS data sets (only available above 4000 m altitude) allowed for deriving the vertical distance (Δh) from RS measurements of their respective height (h_{RS1} and h_{RS2}) as well as the horizontal displacement (Δx) between the geo-positions of both RS. The deflection angle α is then calculatable from Δh, Δx, and the trigonometric function $tan\ \alpha$. In Fig. S 11 the horizontal displacement between RS1 and RS2 is displayed as a function of altitude during the balloon's ascent. The data points are color-coded according to the respective deflection angle α. Mean values of the horizontal displacement ($\overline{\Delta x}$) are shown in the graph together with the standard deviation σ over periods of 60 s each.

Despite disregarding inaccuracies associated with the GPS measurements, the vast majority of data still indicates a horizontal displacement between the balloon and the payload by more than 2.5 m and up 21 m, which strongly indicates that deflection angles up to even beyond 20° with respect to a straight vertical indeed occur during balloon ascents.

Figure S 1: Layout of custom-designed Printed Circuit Board (PCB9), allowing for powering the sensor (by a 12 V DC power supply) and reading the voltage output (U).

Figure S 2: TFS-measured in reference to PPt-measured flow velocities in a flow tube under variable ambient temperatures during a cold chamber test. The mean of 41-78 individual measurements for respective temperature conditions are displayed together with the $1.96 \cdot \sigma$ as vertical bars (co-illustrating the 95 % confidence interval), and with the extremes of ambient temperature scatter throughout the experiments as horizontal bars, a) for TFS 1 and b) for TFS 2.

Figure S 3: Schematic of the wind tunnel used.

Figure S 4: Correlations between flow speeds measured by the calibrated TA (v_{TA}) against those detected by the PPt (v_{PPt}) within the flow tube inside the UCASS for various modifications of the UCASS geometry (Exp. 1 - Exp. 5, see main article Sect. 3.5.1 and Table 1) at seven different ambient flow velocities (each comprising ten single measurements). The standard deviation of measured velocities is given as horizontal bars. Regression fits are applied for each experiment series.

Figure S 5: Experimental setup for comparing the flow velocities inside and outside the UCASS. (a) side view of the test setup, (b) test setup facing against the flow direction from the wind tunnel.

Figure S 6: Comparison of the flow velocities outside and inside the UCASS. Outside, the PPt measures the ambient flow velocity; inside UCASS, the calibrated TFS 8 is installed. Each data point is based on seventeen individual measurements. A first-order polynomial was determined for each of the measurement series. The grey dashed diagonal shows the 1:1 ratio of the flow velocities. The standard deviations are not shown for reasons of clarity.

Figure S 7: Data series of the high-resolution calibration (HRC) of the flow speed measurement with TFS 8. Each calibration point is based on fifteen individual values, from which the mean value and the standard deviation were determined. Resulting calibration curve is also shown.

Figure S 8: Data series of the three-point calibration (TPC) compared to each of the high-resolution calibration (HRC) curves for TFS 8 (a) and TFS 6 (b), respectively. Each data point is based on fifteen individual measurements, from which the mean values were determined and are shown herein; the standard deviations are not shown for reasons of clarity.

Figure S 9: The measurement results when using TFS 7 while repeating the tests previously performed with TFS 8 (see main article Sect. 3.5.4 and 4.3). In Table S 2 corresponding values are provided in tabular form.

Figure S 10: Vertical profiles of the ascent rates based on changed GPS and barometric altitudes per unit time (v_{GPS} and v_{p}, respectively) compared to TFS measurements of the flow velocity (calibration parameters in Table S 3) through two independent UCASS ($v_{\mathrm{TFS1}}^{\mathrm{corr}}, v_{\mathrm{TFS2}}^{\mathrm{corr}}$) of selected balloon soundings during a field mission a) from 04 August, launch at 12:39 (LT), b) from 08 August, launch at 10:36 (LT), c) from 12 August, launch at 09:53 (LT), and d) from 12 August, launch at 16:39 (LT). Ten-seconds-running average of respective data are shown.

Figure S 11: During a balloon sounding (11 July 2023, 14:00 CEST) two radiosondes (RS1 underneath the balloon hull, RS2 as part of the payload) were implied in a balloon-payload-ensemble of ~62 m length in total. The vertical distribution of the horizontal displacement (Δx) between both RS is shown as a function of altitude during ascent. Data points are coloured according to deflection angle α, determined from Δx and height distance Δh between both RS (see Sect. S 4). Mean values ($\overline{\Delta x}$) over 60 s are shown with standard deviation σ.

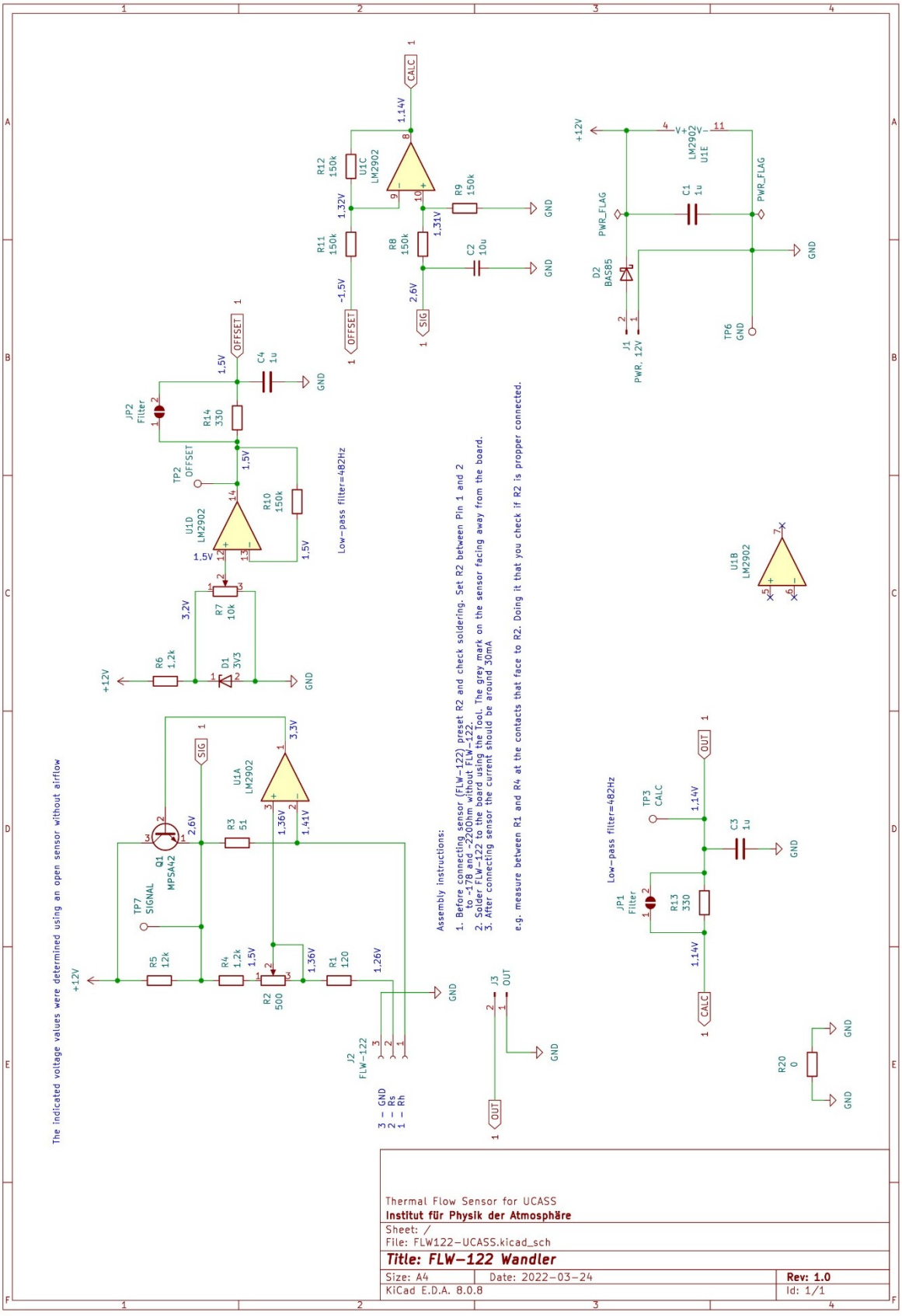
Assembly instructions:
1. Before connecting sensor (FLW-122) preset R2 and check soldering. Set R2 between Pin 1 and 2
should be around 2.2kΩ without FLW-122
2. Solder FLW-122 to the board using the Tool. The grey mark on the sensor facing away from the board.
3. After connecting sensor the current should be around 30mA
e.g. measure between R1 and R4 at the contacts that face to R2. Doing it that you check if R2 is propper connected.
The indicated voltage values were determined using an open sensor without airflow
Low-pass filter=482Hz
Low-pass filter=482Hz
3 - GND
2 - Rs
1 - Rh
Thermal Flow Sensor for UCASS
Institut für Physik der Atmosphäre
Sheet: /
File: FLW122-UCASS.kicad_sch
Title: FLW-122 Wandler
Size: A4
Date: 2022-03-24
Rev: 1.0
KiCad E.D.A. 8.0.8
Id: 1/1

Figure

S 1

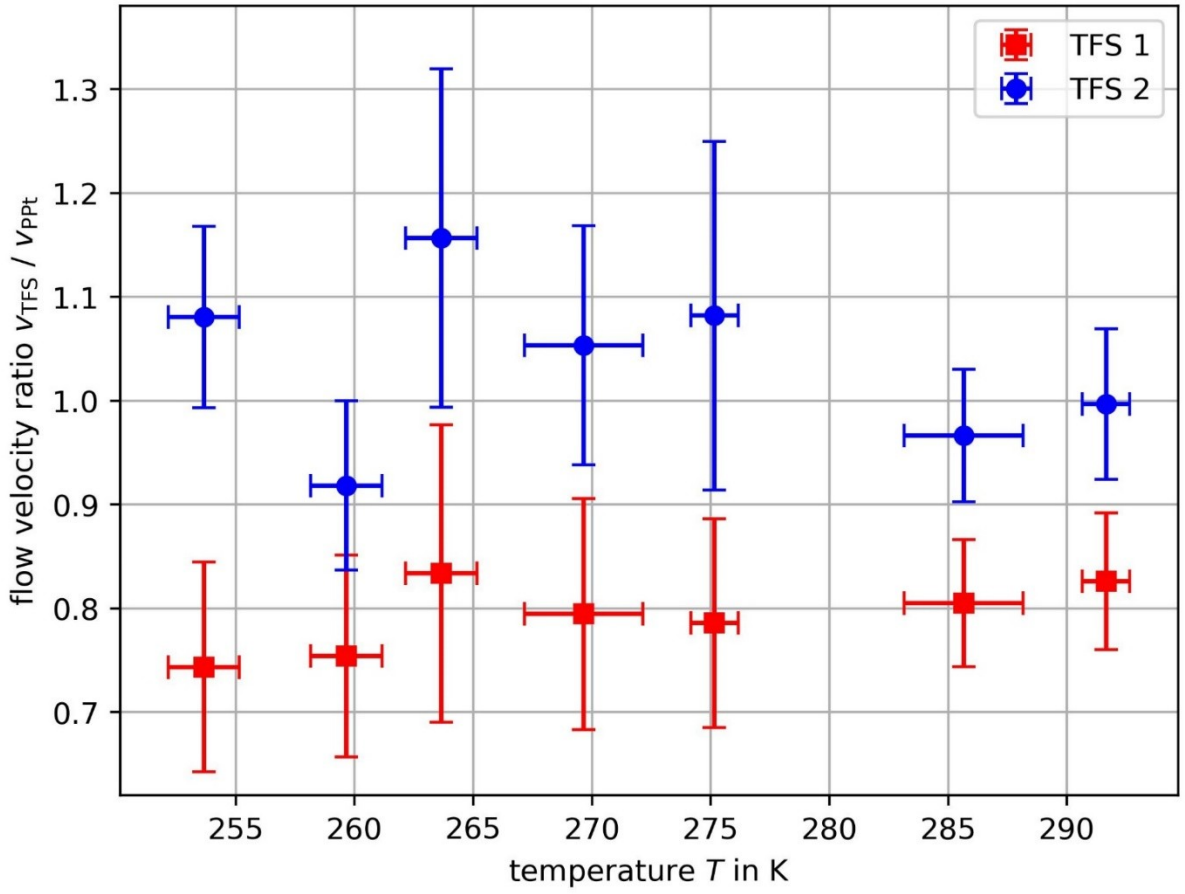
TFS 1
TFS 2
flow velocity ratio v_{TFS} / v_{PPt}
1.3
1.2
1.1
1.0
0.9
0.8
0.7
255
260
265
270
275
280
285
290
temperature T in K

Figure

S 2

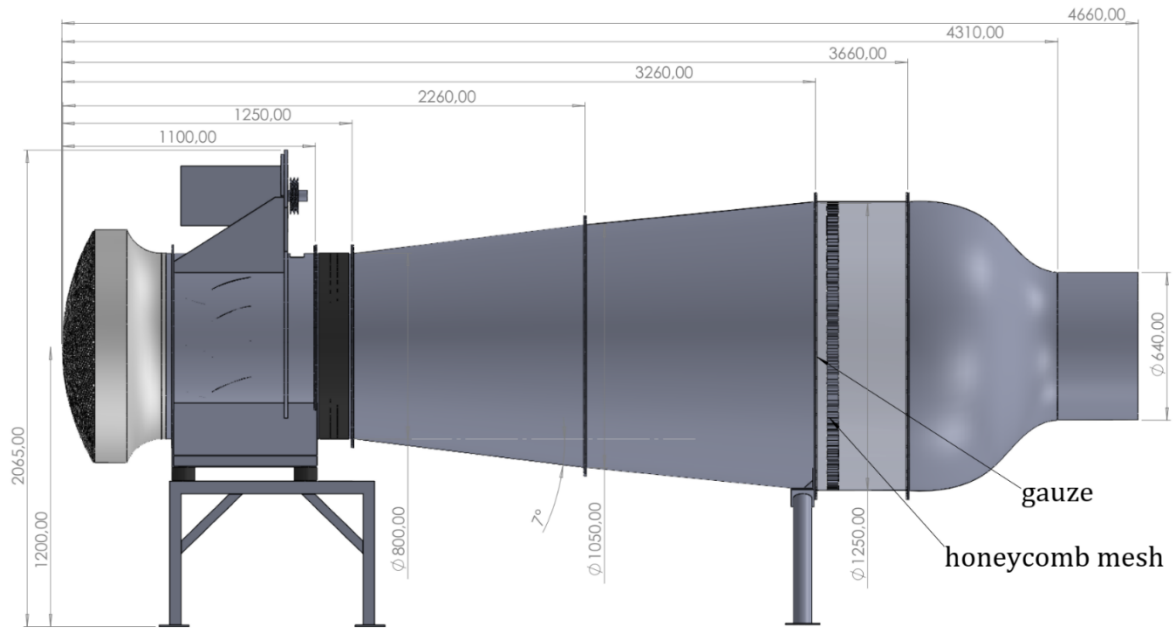
4660,00
4310,00
3660,00
3260,00
2260,00
1250,00
1100,00
2065,00
1200,00
Ø800,00
7°
Ø1050,00
Ø1250,00
Ø640,00
gauze
honeycomb mesh

Figure

S 3

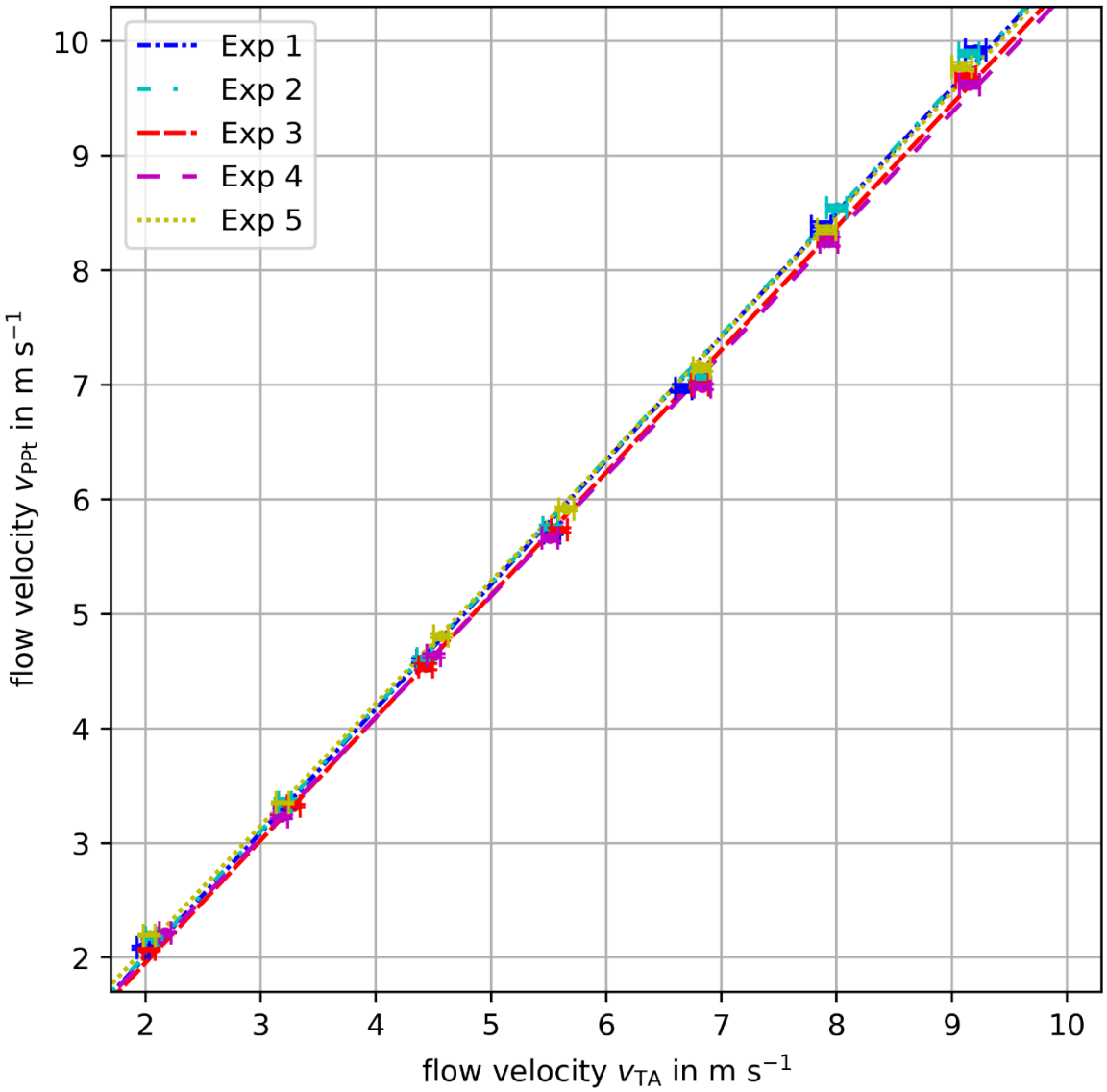
Exp 1
Exp 2
Exp 3
Exp 4
Exp 5
flow velocity v_{PPt} in m s^{-1}
flow velocity v_{TA} in m s^{-1}
2
3
4
5
6
7
8
9
10

Figure

S 4

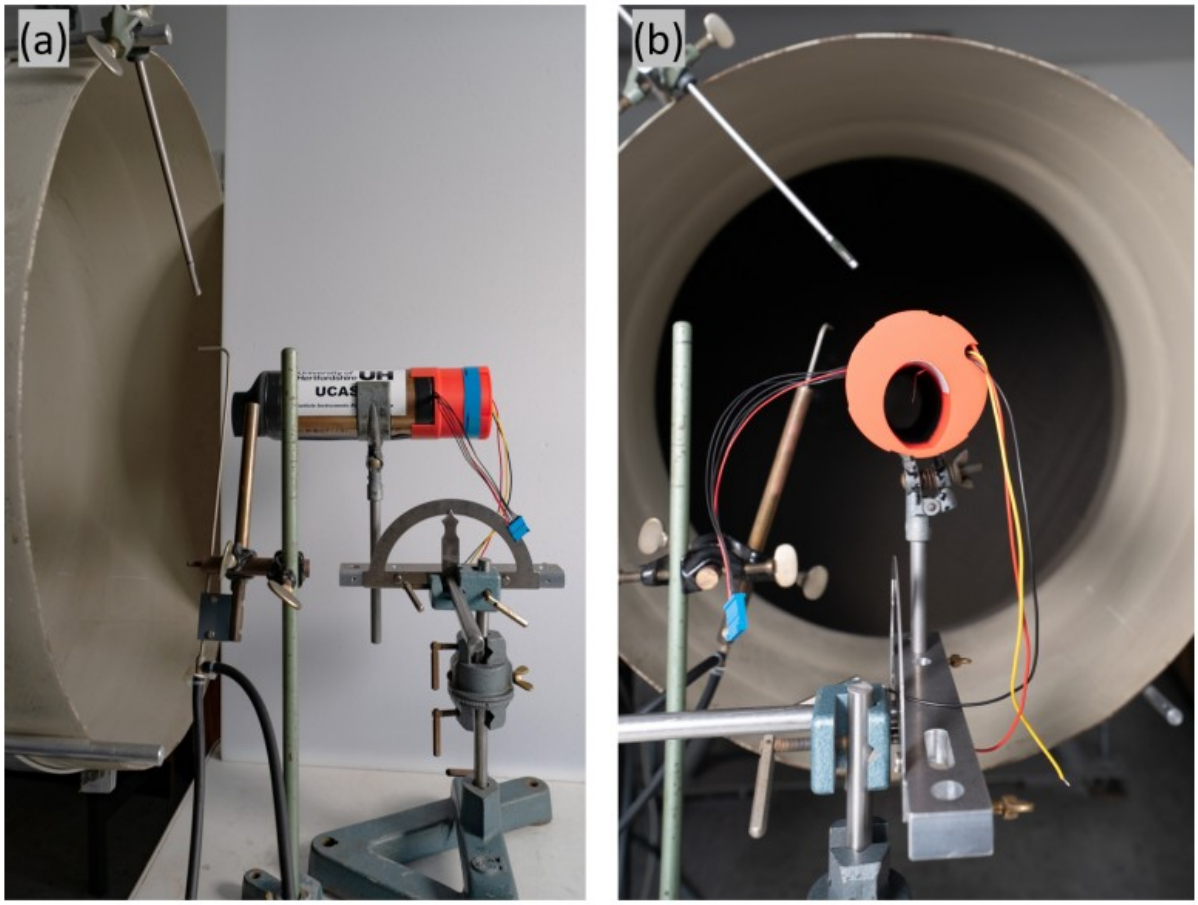

Figure

S 5

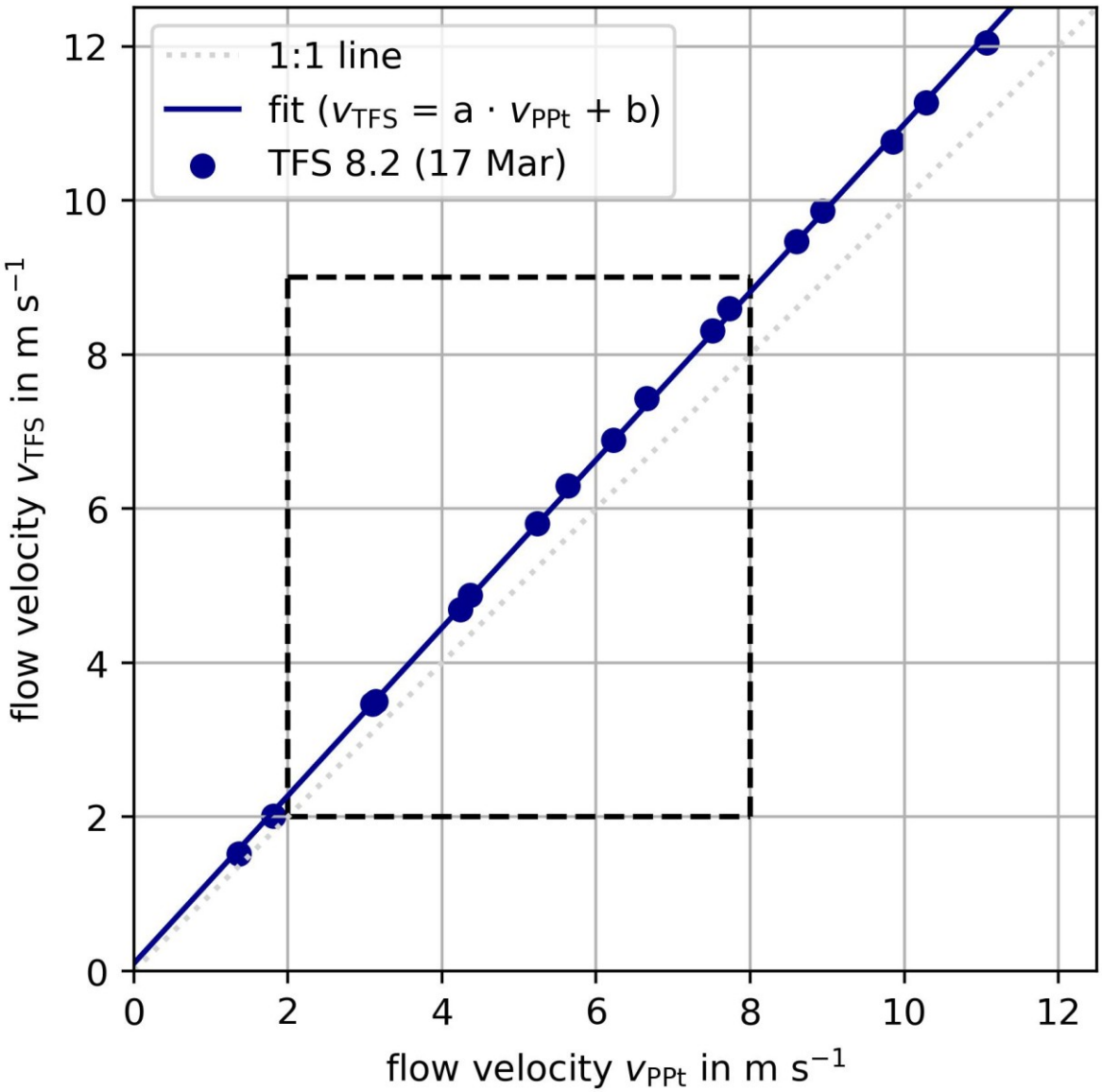
1:1 line
fit (v_{TFS} = a · v_{PPt} + b)
TFS 8.2 (17 Mar)
flow velocity v_{TFS} in m s^{-1}
flow velocity v_{PPt} in m s^{-1}
0
2
4
6
8
10
12

Figure

S 6

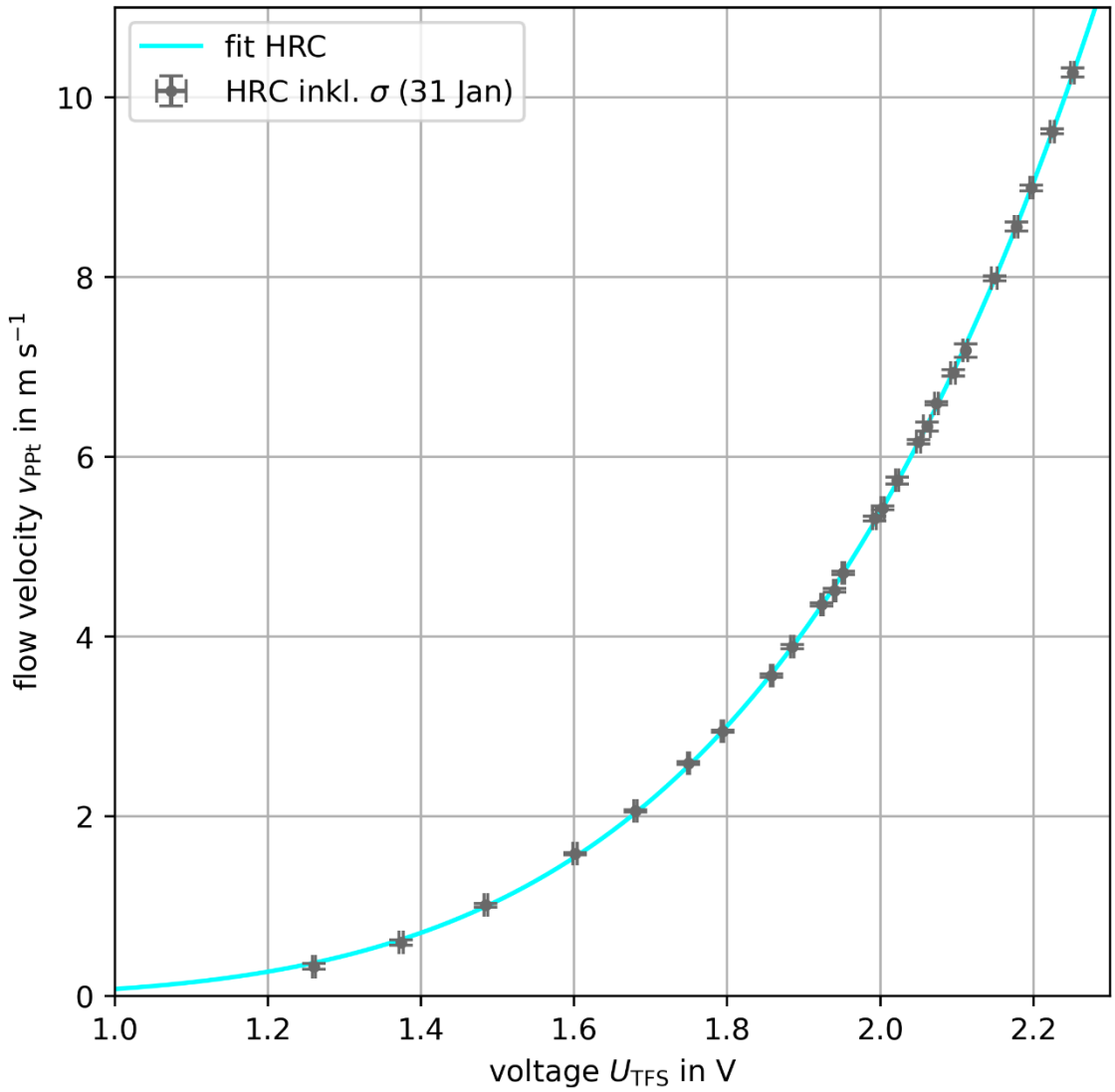
fit HRC
HRC inkl. σ (31 Jan)
flow velocity v_{PPt} in m s^{-1}
voltage U_{TFS} in V
0
2
4
6
8
10
1.0
1.2
1.4
1.6
1.8
2.0
2.2

Figure

S 7

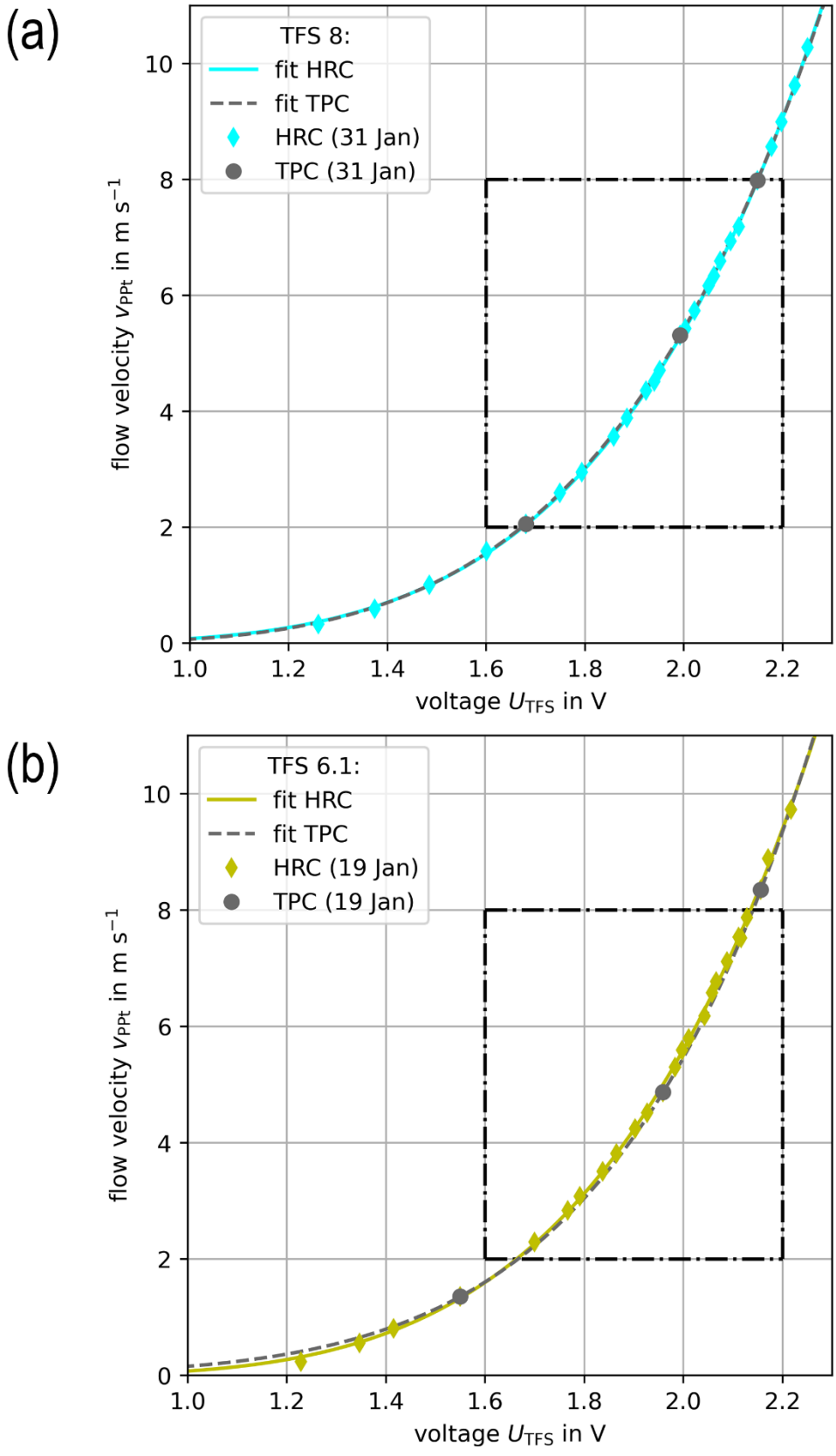
(a)
TFS 8:
fit HRC
fit TPC
HRC (31 Jan)
TPC (31 Jan)
flow velocity v_{PPt} in m s^{-1}
voltage U_{TFS} in V
(b)
TFS 6.1:
fit HRC
fit TPC
HRC (19 Jan)
TPC (19 Jan)
flow velocity v_{PPt} in m s^{-1}
voltage U_{TFS} in V

Figure

S 8

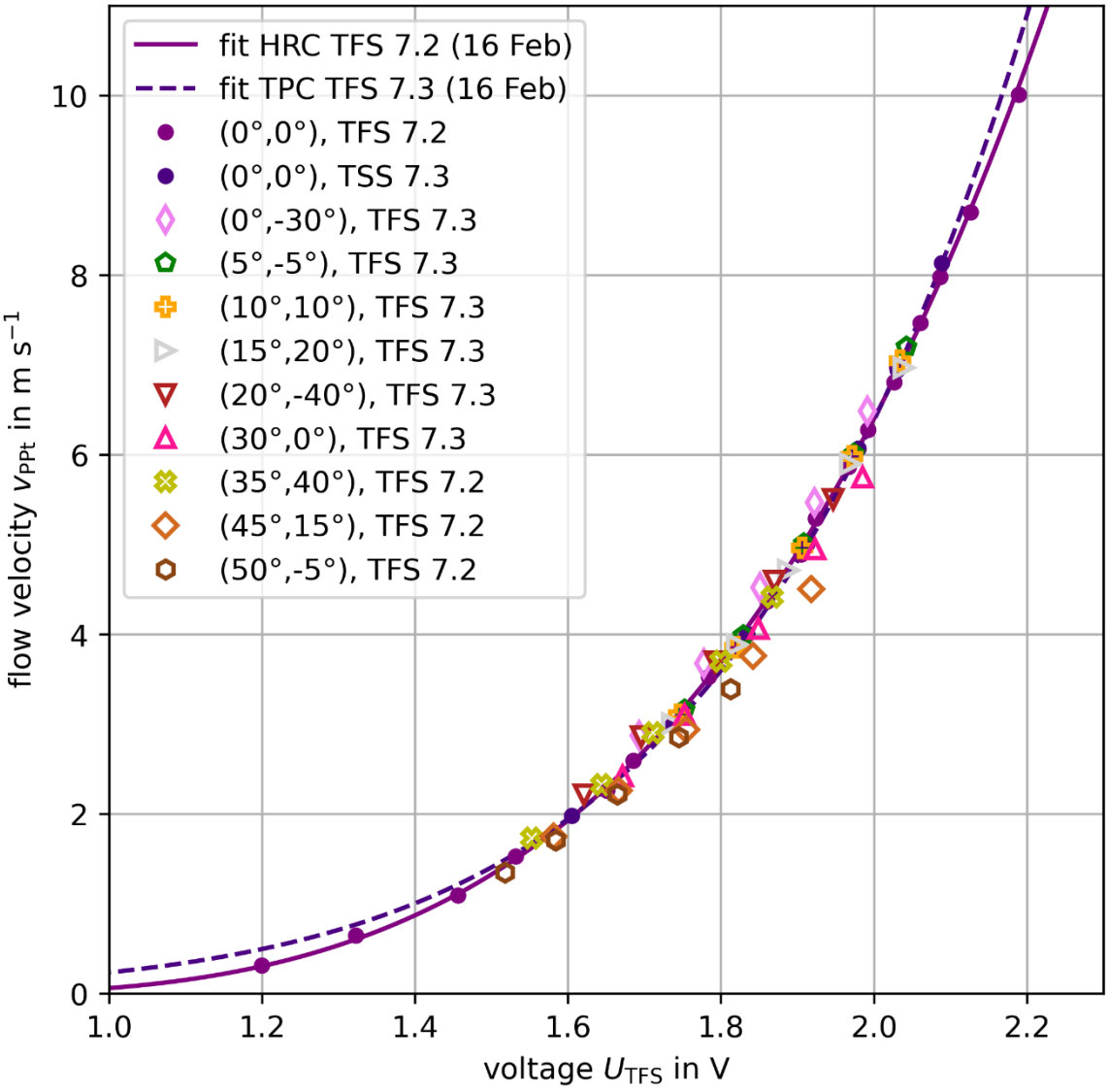
fit HRC TFS 7.2 (16 Feb)
fit TPC TFS 7.3 (16 Feb)
(0°,0°), TFS 7.2
(0°,0°), TSS 7.3
(0°,-30°), TFS 7.3
(5°,-5°), TFS 7.3
(10°,10°), TFS 7.3
(15°,20°), TFS 7.3
(20°,-40°), TFS 7.3
(30°,0°), TFS 7.3
(35°,40°), TFS 7.2
(45°,15°), TFS 7.2
(50°,-5°), TFS 7.2
flow velocity v_{PPt} in m s^{-1}
voltage U_{TFS} in V
0
2
4
6
8
10
1.0
1.2
1.4
1.6
1.8
2.0
2.2

Figure

S 9

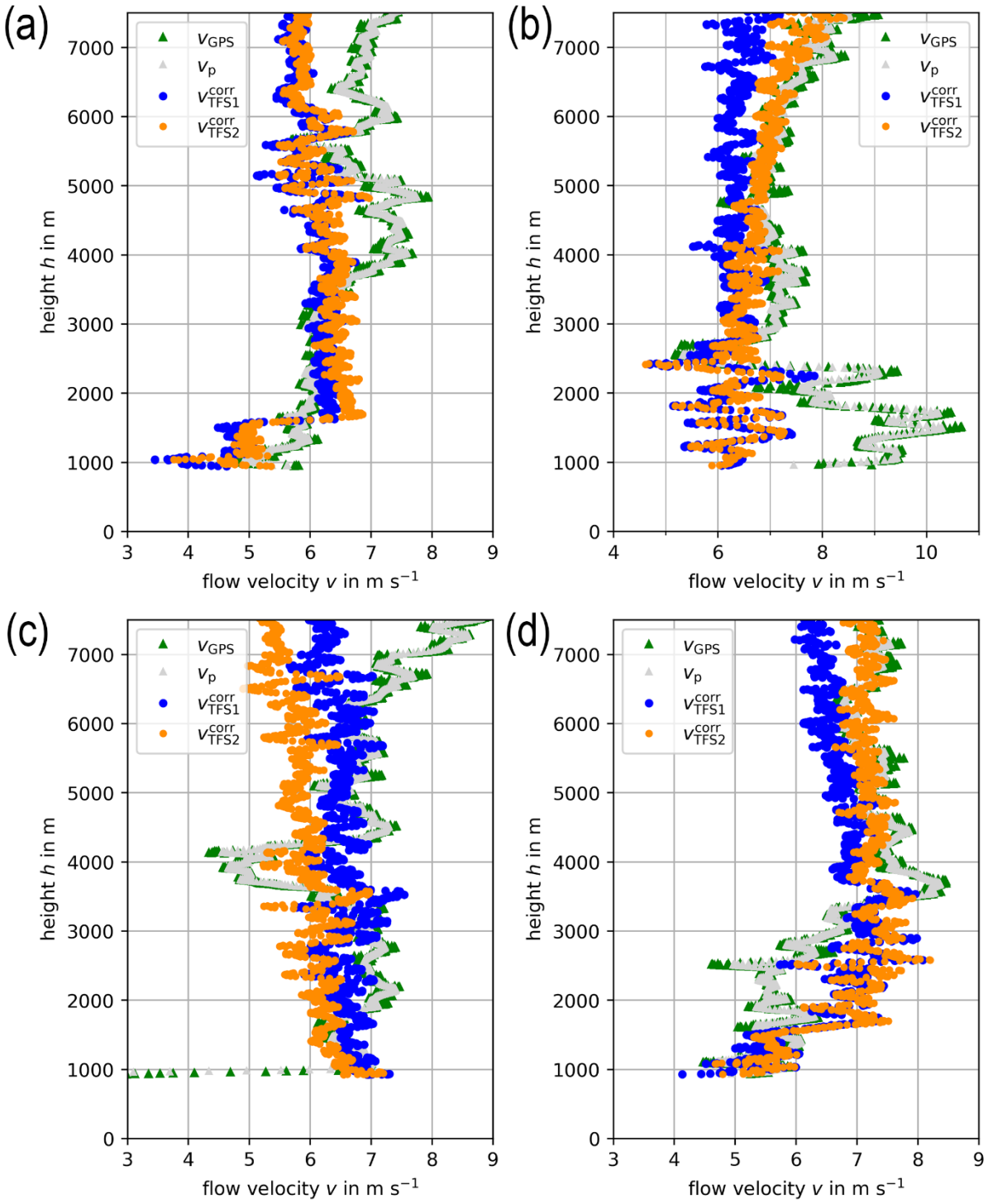
(a)
(b)
(c)
(d)
v_{GPS}
v_p
v_{TFS1}^{corr}
v_{TFS2}^{corr}
height h in m
flow velocity v in m s^{-1}

Figure

S 10

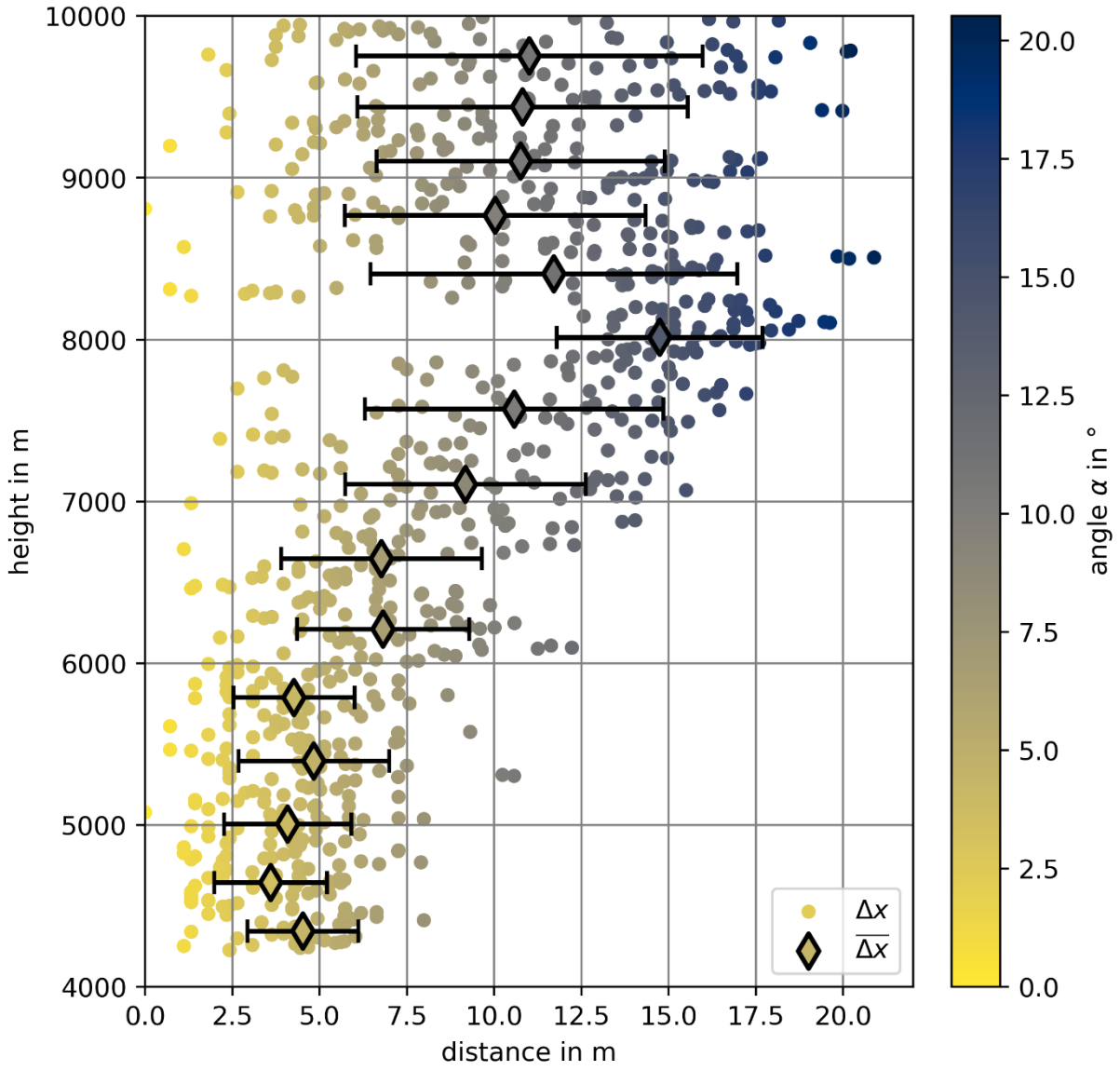
10000
9000
8000
7000
6000
5000
4000
height in m
0.0
2.5
5.0
7.5
10.0
12.5
15.0
17.5
20.0
distance in m
Δx
Δx
20.0
17.5
15.0
12.5
10.0
7.5
5.0
2.5
0.0
angle α in °

Figure

S 11

Parameterisation: $\boldsymbol{v}_{\mathrm{TFS}} = \left(\frac{\mathbf{1}}{\boldsymbol{B}} \cdot \left(\boldsymbol{U^2} - \boldsymbol{A}\right)\right)^{\frac{\mathbf{1}}{\boldsymbol{N}}}$

TFS number	*B*	*A*	*N*
1	1.380	0.709	0.461
2+2.1	1.867	0.110	0.369
4	1.696	0.119	0.398
4.1	1.631	0.181	0.409
4+4.1	1.650	0.164	0.406
4.2	2.018	-0.210	0.348
4.3	1.895	-0.097	0.367
5	1.195	0.977	0.544
6	1.724	0.452	0.409
6.1	1.819	0.364	0.402
6.1 (TPC)	2.485	-0.344	0.329
7.1	1.790	0.240	0.392
7.2	1.451	0.597	0.459
7.3 (TPC)	2.666	-0.711	0.307
8	1.898	0.309	0.395
8 (TPC)	1.789	0.417	0.411
8.1 (TPC)	1.711	0.512	0.426
8.2 (TPC)	2.055	0.136	0.384
9	1.150	1.112	0.570

Table S 1

Coefficients *A* in V^2, *B* in V^2 s m^{-1} and *N* (dimensionless) of the calibration curves for individual TFS calibrated (TPC = Three-point calibration).

angle (φ, ϑ)	calibration curve	deviation $\Delta v_{\mathrm{rel}}^{\mathrm{max}}$ in %	deviation $\Delta \bar{v}_{\mathrm{rel}}$ in %
(0°,-30°)	TFS 7.3	10.5	7.7
(5°,-5°)	TFS 7.3	1.7	1.3
(10°, 10°)	TFS 7.3	1.5	1.2
(15°, 20°)	TFS 7.3	1.8	1.3
(20°,-40°)	TFS 7.3	8.9	4.9
(30°, 0°)	TFS 7.3	6.1	2.6
(35°, 40°)	TFS 7.2	6.7	3.1
(45°, 15°)	TFS 7.2	12.6	8.2
(50°,-5°)	TFS 7.2	11.4	7.8

Table S 2

Maximum ($\Delta v_{\mathrm{rel}}^{\mathrm{max}}$) and mean values ($\Delta \bar{v}_{\mathrm{rel}}$) of the percentual relative deviation of measured flow velocities under variable angle of attack (AOA) for the calibration curve of TFS 7 (cf. Fig. S 9).

Balloon soundings	TFS	*B*	*A*	*N*
20240812_1410 (LT)	#33	2.273	0.055	0.374
(Fig. 7, main article)	#34	2.292	0.050	0.379
20240816_1151 (LT)	#31	2.276	-0.320	0.340
(Fig. 7, main article)	#32	2.250	-0.105	0.356
20240816_1341 (LT)	#3	2.718	-0.375	0.334
(Fig. 7, main article)	#4	3.363	-1.136	0.276
20240804_1239 (LT)	#17	2.313	-0.064	0.359
(Fig. S 10)	#18	2.563	-0.256	0.341
20240808_1036 (LT)	#5	3.528	-1.296	0.271
(Fig. S 10)	#6	2.146	0.011	0.379
20240812_0953 (LT)	#27	2.261	-0.236	0.349
(Fig. S 10)	#28	2.291	0.022	0.368
20240812_1639 (LT)	#21	3.117	-0.882	0.295
(Fig. S 10)	#22	2.532	-0.375	0.331

Table S 3

Coefficients *A* in V^2, *B* in V^2 s m^{-1} and *N* (dimensionless) of the calibration curves for individual TFS calibrated. The vertical profiles calculated from the parameters are shown in Fig. 7 (main article) and Fig. S 10 (herein).